EPJ manuscript No.
(will be inserted by the editor)

Improving Robustness of Complex Networks via the Effective Graph Resistance

Xiangrong Wang[1], Evangelos Pournaras[1], Robert E. Kooij[12], and Piet Van Mieghem[1]

[1] Faculty of Electrical Engineering, Mathematics and Computer Science, Delft University of Technology, Delft, The Netherlands, e-mail: {X.Wang-2, R.E.Kooij, E.Pournaras, P.F.A.VanMieghem}@tudelft.nl.
[2] TNO, Delft, The Netherlands.

Received: date / Revised version: date

Abstract. Improving robustness of complex networks is a challenge in several application domains, such as power grids and water management networks. In such networks, high robustness can be achieved by optimizing graph metrics such as the effective graph resistance, which is the focus of this paper. An important challenge lies in improving the robustness of complex networks under dynamic topological network changes, such as link addition and removal. This paper contributes theoretical and experimental findings about the robustness of complex networks under two scenarios: (i) selecting a link whose addition maximally decreases the effective graph resistance; (ii) protecting a link whose removal maximally increases the effective graph resistance. Upper and lower bounds of the effective graph resistance under these topological changes are derived. Four strategies that select single links for addition or removal, based on topological and spectral metrics, are evaluated on various synthetic and real-world networks. Furthermore, this paper illustrates a novel comparison method by considering the distance between the added or removed links, optimized according to the effective graph resistance and the algebraic connectivity. The optimal links are different in most cases but in close proximity.

1 Introduction

Several complex infrastructural networks are built to geographically distribute flows of critical resources for our society. Electrical networks, via power lines, and water/gas networks, via pipe lines, are representative examples. In the lines of these networks, opposition forces, governed by physical laws[1], resist the passage of electric current or water/gas molecules. It is shown that these physical characteristics of resistance in individual lines play a key role in the robustness of the network as a whole [1–3], e.g., network robustness under cascading failures [4].

This paper studies the graph metric of *effective graph resistance* as a robustness measure of complex networks. The effective graph resistance can be measured in graphs, therefore, it is a robustness indicator for several real-world networks that can be modeled as graphs. Ellens *et al*. [1] show that the lower the effective graph resistance is, the more robust a network is. Adding a link reduces the effective graph resistance and thus improves the robustness of a network. This scenario is applicable to infrastructural investments that shall increase system lifetime by installing single lines. On the other hand, removing a link increases the effective graph resistance. The robustness is improved by 'protecting' the link whose removal maximally increases the effective graph resistance. This scenario is applicable to cyber-physical targeted attacks of infrastructural lines. The challenge in both scenarios lies in the selection of a link, among all the possible ones, whose addition or removal maximally decreases or increases the effective graph resistance.

Earlier work studies the effective graph resistance in networks that are topologically changed. For example, Ghosh *et al*. [5] study the minimization of the effective graph resistance by allocating link weights in weighted graphs. Van Mieghem *et al*. [6] show the relation between the effective graph resistance and the linear degree correlation coefficient. Abbas *et al*. [3] reduce the effective graph resistance of a graph by adding links in a step-wise way. In contrast to the aforementioned approaches, this paper focuses on the effective graph resistance as an indicator of robustness in complex networks when single links are added or removed.

The contributions of this paper are the following: (i) Theorems that prove upper and lower bounds of the effective graph resistance. (ii) Optimization strategies that are experimentally evaluated under synthetic and real-world networks. These strategies maximize the decrease or the increase of effective graph resistance under link addition and removal respectively. (iii) A method and experimental results that topologically compare the optimal added or removed links according to effective graph resistance and algebraic connectivity. Therefore, this paper provides a broad spectrum of theoretical and experimental findings on effective graph resistance as an indicator of robustness in synthetic and real-world networks.

[1] The Ohm's law for electrical networks and the Poiseuille's law for water networks.

This paper is organized as follows: Section 2 defines the effective graph resistance and summarizes its properties. Section 3 derives bounds of the effective graph resistance under link addition and removal. The design and evaluation of the four strategies are illustrated in Section 4. The comparison between the optimization of the effective graph resistance and the algebraic connectivity is investigated in Section 5. Section 6 compares the optimization of the effective graph resistance with other approaches in related work. Section 7 concludes the paper and outlines future work.

2 Effective graph resistance in Complex Networks

Let $G(N, L)$ be an undirected graph with N nodes and L links. Adding or removing a link $e = i \sim j$ results in a graph $G + \{e\}$ or $G - \{e\}$. The adjacency matrix A of a graph G is an $N \times N$ symmetric matrix with elements a_{ij} that are either 1 or 0 depending on whether there is a link between nodes i and j or not. The Laplacian matrix Q of G is an $N \times N$ symmetric matrix $Q = \Delta - A$, where Δ =diag(d_i) is the $N \times N$ diagonal degree matrix with the elements $d_i = \sum_{j=1}^{N} a_{ij}$. The average degree in G is denoted as $E[D] = \frac{2L}{N}$. The Laplacian eigenvalues of Q are all real and non-negative [7]. The eigenvalues of Q are ordered as $0 = \mu_N \leq \mu_{N-1} \leq \ldots \leq \mu_1$. The second lowest eigenvalue $\mu_{N-1} = \alpha_G$ is coined by Fielder [8] as the algebraic connectivity. In this paper, the effective graph resistance R_G is computed as follows [7]:

$$R_G = N \sum_{i=1}^{N-1} \frac{1}{\mu_i} \tag{1}$$

In order to compare the effective graph resistance R_G between networks with different size, the value of the effective graph resistance in Section 4 is normalized by dividing R_G with $\binom{N}{2}$.

An alternative normalization approach is the normalized *effective graph conductance* defined as follows:

$$C^* = \frac{N-1}{R_G} \tag{2}$$

The values of C^* lie in the interval $[0, 1]$ that follows from the general inequality [7]:

$$R_G \geq \frac{(N-1)^2}{E[D]} \tag{3}$$

where $E[D] \leq N - 1$. For the complete graph, it holds that $C^* = 1$, whereas for disconnected graphs, it holds that $C^* = 0$. This paper focuses on the first normalization method that is closer to the concept of effective graph resistance.

The improvement of robustness via the effective graph resistance consists of two parts: adding an optimal link l_{R^+} that minimizes the effective graph resistance $R_{G+\{e\}}$ and protecting the link l_{R^-} whose removal maximizes the effective graph resistance $R_{G-\{e\}}$. The effective graph resistance strictly decreases if a link is added into a graph and strictly increases if a link is removed from a graph[2][1, 9]. A strategy in this work refers to the addition of a single link $e = i \sim j$ according to a specific rule, with the aim to minimize the effective graph resistance of the graph $G + \{e\}$. The total number of possible links are:

$$L_c = \binom{N}{2} - L \tag{4}$$

A strategy also selects a link to protect from all the possible links L whose removal maximally increases the effective graph resistance.

The comparison between the optimal link l_{R^+} for the effective graph resistance $R_{G+\{e\}}$ and the optimal link l_{α^+} for the algebraic connectivity $\alpha_{G+\{e\}}$ is based on two computations. The two computations are also performed for the comparison between optimal links l_{R^-} and l_{α^-}.

The first computation calculates the probability that the two optimal links are the same link. From the definition (1) of the effective graph resistance R_G, the algebraic connectivity α_G can be written as $\alpha_G = \mu_{N-1} = \frac{1}{R_G/N - S}$, where $S = \sum_{k=1}^{N-2} \frac{1}{\mu_k}$. Based on the definition of S, an upper and lower bound of the algebraic connectivity in terms of the effective graph resistance is derived in the Appendix A. When S is negligibly low, the two optimal links for the algebraic connectivity α_G and for the effective graph resistance R_G are the same link with probability $\Pr[l_{R^+} = l_{\alpha^+}]$ for link addition and $\Pr[l_{R^-} = l_{\alpha^-}]$ for link removal.

The second computation concerns the distance between l_{R^+} and l_{α^+} when they are not the same link with probability $1-\Pr[l_{R^+} = l_{\alpha^+}]$. The distance between links in a graph G is measured by the hopcount in the corresponding line graph G^*. A line graph G^* of a graph G is a graph in which every node of G^* corresponds to a link in G and two nodes of G^* are adjacent if and only if the corresponding links in G have a node in common [7]. The graph G is referred to as the root graph of G^*. The links l_{R^+} and l_{α^+} in the root graph G are denoted as the nodes n_{R^+} and n_{α^+} in the line graph G^*. The hopcount $H(n_{R^+}, n_{\alpha^+})$ in G^* is the number of links in the shortest path between nodes n_{R^+} and n_{α^+}. The probability $\Pr[H(n_{R^+}, n_{\alpha^+}) = 0]$ equals to the probability $\Pr[l_{R^+} = l_{\alpha^+}]$. The hopcount $H(n_{R^+}, n_{\alpha^+}) = 1$ means that the link l_{R^+} and the link l_{α^+} share a common node.

Table 1 illustrates the mathematical symbols used in this paper.

The complex networks in which this paper focuses on include synthetic and real-world networks. Synthetic networks are as follows[3]:

Erdős-Rényi random graph [10] $G_p(N)$**:** This graph is generated from a set of N nodes by randomly assigning a link between each node pair with probability p. The probability p is also called the link density. When the link

[2] This is also confirmed by Section 3 based on interlacing [7].

[3] All these listed networks are converted to undirected and unweighted connected networks.

Table 1: An overview of the mathematical symbols

Symbol	Interpretation
G	A graph
N	Number of nodes in a graph G
L	Number of links in a graph G
e	A link in a graph G
A	Adjacency matrix
a_{ij}	An element in the adjacency matrix A
d_i	Degree of a node i
Δ	Diagonal matrix with the nodal degrees
Q	Laplacian matrix
$E[D]$	Average degree
μ_i	Eigenvalue of the Laplacian matrix
α_G	Algebraic connectivity
R_G	Effective graph resistance for a graph G
C^*	Effective graph conductance
$R_{G+\{e\}}$	Effective graph resistance for $G+\{e\}$
$R_{G-\{e\}}$	Effective graph resistance for $G-\{e\}$
l_{R^+}	Optimal link whose addition minimizes R_G
l_{R^-}	Optimal link whose removal maximizes R_G
l_{α^+}	Optimal link whose addition maximizes α_G
l_{α^-}	Optimal link whose removal minimizes α_G
L_c	Number of possible links for link addition
G^*	Line graph of a graph G
n_{R^+}	Node in line graph corresponding to l_{R^+}
n_{R^-}	Node in line graph corresponding to l_{R^-}
n_{α^+}	Node in line graph corresponding to l_{α^+}
n_{α^-}	Node in line graph corresponding to l_{α^-}
$H(n_{R^+}, n_{\alpha^+})$	Hopcount between n_{R^+} and n_{α^+}
$H(n_{R^-}, n_{\alpha^-})$	Hopcount between n_{R^-} and n_{α^-}
$\Delta\mu_i$	Increase or decrease of an eigenvalue μ_i
ρ	Diameter of a graph G
S_s	A strategy s
y	Fiedler vector
R_{ij}	Effective resistance between nodes i and j
Q^{-1}	Moore-Penrose pseudoinverse of Q
cc_i	Closeness centrality of a node i
H_{ij}	Hopcounts from a node i to a node j
$G_p(N)$	An Erdős-Rényi graph
p	Link density
$E[H]$	Average hopcount
R_{D_s}	Relative difference of R_G
$E[R_{D_s}]$	Average of R_{D_s}

density p is higher than a critical threshold $p_c \approx \ln N/N$, the graph is connected [11].

Barabási-Albert power law graph [12]: This graph is generated by starting with m nodes. At every time step, a new node with m links is connected to the m existing nodes in the network. A new node connects to a node i in step t with probability $p = d_i/2L_t$, where d_i is the degree of node i and L_t is the total number of links at time t.

Watts-Strogatz small-world graph [13]: This graph is generated from a ring lattice of N nodes and k links per node. Each link is rewired at random with probability p.

These graph models have characteristics found in real-world networks. For example, Erdős-Rényi graphs can model collaboration networks [14]. The world-wide web follows approximately a power law degree distribution [15]. Social networks are often connected as small world networks [13].

In this paper the following real-world networks are considered:

Dutch Soccer Network [16]: A graph of the Dutch football in which players represent the nodes. Two nodes are connected if the corresponding two players have played together in a football match.

Coauthorship Network of Scientists [17]: Scientists are nodes and two scientists are considered connected if they are authors in one or more papers.

Protein-Protein Interaction Network[4]**:** The nodes are proteins and the links are pairwise protein-to-protein interactions.

Citation Network[5]**:** The nodes are scientific papers and the links between the nodes are citations.

Western States Power Grid Network [18]: The nodes represent transformers, substations and generators. The links represent high-voltage transmission lines.

Western European Railway Network [18]: The stations are the nodes and the links are lines between the stations.

3 Theoretical Bounds

Topological network changes influence various graph metrics such as the effective graph resistance and algebraic connectivity studied in this paper. Upper and lower theoretical bounds measure the highest and lowest values that a graph metric can have after certain topological network changes. Therefore, bounds can be used to reason about robustness estimations under topological changes such as link addition or removal. Bounds provide valuable estimations in various application domains. For example, the upper and lower bounds of throughput instruct the design of a wireless network in which node connections follow mobility patterns [19]. Another example is the estimation of interference by upper and lower bounds when nodes are clustered in Ad Hoc Networks [20].

3.1 Link Addition

After adding a link e, resulting in a graph $G+\{e\}$, a lower bound of the effective graph resistance $R_{G+\{e\}}$ is derived in Theorem 1. An upper bound $R_{G+\{e\}} \leq R_G$ is obtained in the proof of Theorem 1 based on interlacing [7].

Theorem 1. *By adding a link e to a graph G, resulting in the graph $G+\{e\}$, the lower bound of the effective graph resistance $R_{G+\{e\}}$ is*

$$R_{G+\{e\}} \geq \frac{R_G}{1+\frac{\rho}{2}N} \tag{5}$$

where ρ is the diameter of G.

[4] http://www.pdb.org/pdb/home/home.do (Last accessed: Apr. 2014).

[5] http://vlado.fmf.uni-lj.si/pub/networks/data/ (Last accessed: Apr. 2014).

Proof.. The sum of Laplacian eigenvalues equals [7]

$$\sum_{j=1}^{N-1} \mu_j = 2L$$

After a link addition, graph G has $L+1$ links and it holds that $\sum_{j=1}^{N-1}(\mu_j + \Delta\mu_j) = 2(L+1)$. The increase of the eigenvalue $\Delta\mu_j$ satisfies $\sum_{j=1}^{N-1}\Delta\mu_j = 2(L+1) - \sum_{j=1}^{N-1}\mu_j = 2(L+1) - 2L = 2$. Interlacing [7] $\mu_j \leq \mu_j + \Delta\mu_j \leq \mu_{j-1}$ shows that $\Delta\mu_j \geq 0$ for any j, so that $\Delta\mu_j \leq 2$. For positive real numbers q_1, q_2,..., q_n and real numbers a_1, a_2,..., a_n, it holds [7]

$$\min_{1\leq k\leq n}\frac{x_k}{a_k} \leq \frac{x_1+x_2+\ldots+x_n}{a_1+a_2+\ldots+a_n} \leq \max_{1\leq k\leq n}\frac{x_k}{a_k} \qquad (6)$$

Let $x_j = \frac{1}{\mu_j+\Delta\mu_j}$ and $a_j = \frac{1}{\mu_j}$. Based on the definition (1) of the effective graph resistance, inequality (6) yields

$$\frac{1}{1+\max_{1\leq j\leq N-1}\frac{\Delta\mu_j}{\mu_j}} \leq \frac{\sum_{j=1}^{N-1}\frac{1}{\mu_j+\Delta\mu_j}}{\sum_{j=1}^{N-1}\frac{1}{\mu_j}} = \frac{R_{G+\{e\}}}{R_G} \leq 1$$

Furthermore, with $\max_{1\leq j\leq N-1}\frac{\Delta\mu_j}{\mu_j} \leq \frac{2}{\mu_{N-1}}$ and the lower bound [7] for the algebraic connectivity $\mu_{N-1} \geq \frac{4}{\rho N}$, the lower bound of (5) is derived. □

A consequence of the lower bound (5) is $\frac{R_{G+\{e_1\ldots e_m\}}}{R_G} \geq \left(1+\frac{m\rho}{2}N\right)^{-1}$ after m repeated link additions. In particular, a graph G can always be constructed by starting from its minimum spanning tree and adding $L-N+1$ links. Given that the effective graph resistance $R_{MST} = \binom{N}{2}E[H_{MST}]$ for a minimum spanning tree [7], where H_{MST} is the hopcount in any minimum spanning tree, the lower bound of the effective graph resistance can be expressed as follows:

$$R_G \geq \frac{R_{MST}}{1+\frac{\rho_{MST}}{2}N(L-N+1)} = \frac{\binom{N}{2}E[H_{MST}]}{1+\frac{\max H_{MST}}{2}N(L-N+1)}$$

This bound may be valuable in sparse networks where L is not significantly larger than $N-1$.

Figure 1 shows the lower bound of the effective graph resistance $R_{G+\{e\}}$ from Theorem 1 in Erdős-Rényi, Barabási-Albert and square lattice[6] graphs. The lower bound is not tight, yet, a sharper lower bound can be derived by using the algebraic connectivity μ_{N-1} in the lower bound $\frac{R_G}{1+\frac{2}{\mu_{N-1}}}$. Figure 1 also shows the improved lower bound based upon the algebraic connectivity. This observation and the proof followed here suggest that the lower bound (5) can be improved with a sharper lower bound for the algebraic connectivity.

[6] The square lattice graph is a two-dimensional grid. Excluding the boundary nodes, the square lattice can be regarded as a regular graph with degree $d = 4$.

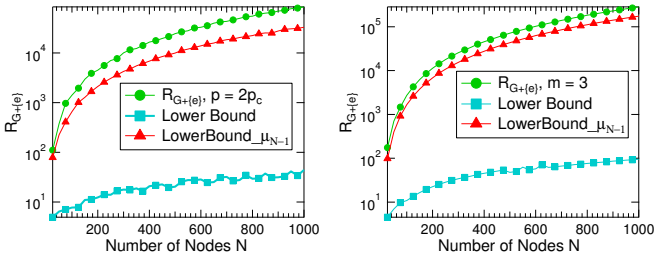

(a) Erdős-Rényi graph (b) Barabási-Albert graph

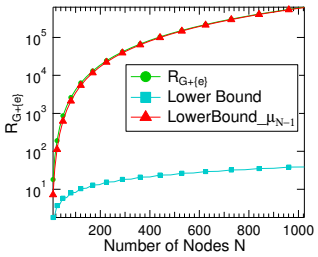

(c) Square lattice graph

Fig. 1: Lower bounds of the effective graph resistance $R_{G+\{e\}}$.

3.2 Link Removal

When a link e is removed from a graph, a lower bound of the effective graph resistance $R_{G-\{e\}}$ is derived in Theorem 2 and an upper bound in Theorem 3.

Theorem 2. *By removing a link e from a graph G, resulting in a reduced graph $G-\{e\}$, the lower bound of the effective graph resistance $R_{G-\{e\}}$ of the reduced graph $G-\{e\}$ is*

$$R_{G-\{e\}} \geq \frac{N(N-1)(N+1)}{2(L-1)} \qquad (7)$$

where N is the number of nodes and L is the number of links of the original graph G.

Proof.. Let $\Delta\mu_i$ defined as the amount of the decrease of an eigenvalue μ_i. The effective graph resistance $R_{G-\{e\}}$ of the reduced graph $G-\{e\}$ is

$$R_{G-\{e\}} = N\sum_{i=1}^{N-1}\frac{1}{\mu_i-\Delta\mu_i} = N\left(\frac{1}{\mu_{N-1}-\Delta\mu_{N-1}} + \sum_{i=1}^{N-2}\frac{1}{\mu_i-\Delta\mu_i}\right) \qquad (8)$$

For positive real numbers a_1, a_2, ..., a_n, the harmonic, geometric and arithmetic mean inequality [7] is

$$\frac{n}{\sum_{k=1}^{n}\frac{1}{a_k}} \leq \sqrt[n]{\prod_{k=1}^{n}a_k} \leq \frac{1}{n}\sum_{k=1}^{n}a_k \qquad (9)$$

with equality only if all a_k are equal. Let a_1, a_2, ..., a_n be equivalent to $\mu_{N-2}-\Delta\mu_{N-2}$, $\mu_{N-3}-\Delta\mu_{N-3}$, ..., $\mu_1-\Delta\mu_1$

and $n = N-2$. Inequality (9) is expressed as follows:

$$\frac{N-2}{\sum_{i=1}^{N-2}\frac{1}{\mu_i-\Delta\mu_i}} \leq \frac{1}{N-2}\sum_{i=1}^{N-2}(\mu_i-\Delta\mu_i) \tag{10}$$

Taking the reciprocal and then multiplying $N-2$ on both sides of the inequality (10) yields

$$\begin{aligned}\sum_{i=1}^{N-2}\frac{1}{\mu_i-\Delta\mu_i} &\geq \frac{(N-2)^2}{\sum_{i=1}^{N-2}(\mu_i-\Delta\mu_i)} \\ &= \frac{(N-2)^2}{2(L-1)-(\mu_{N-1}-\Delta\mu_{N-1})}\end{aligned} \tag{11}$$

where the sum of eigenvalues satisfies $\sum_{i=1}^{N-1}(\mu_i-\Delta\mu_i) = 2(L-1)$. Substituting the inequality (11) into (8) yields

$$\begin{aligned}R_{G-\{e\}} \geq & N\Big(\frac{1}{\mu_{N-1}-\Delta\mu_{N-1}} \\ &+ \frac{(N-2)^2}{2(L-1)-(\mu_{N-1}-\Delta\mu_{N-1})}\Big)\end{aligned}$$

Since the function, for $x > 0$,

$$f(x) = \frac{1}{x} + \frac{(N-2)^2}{2(L-1)-x}$$

has a unique minimum at the positive value $x = \frac{2(L-1)}{N-1}$, it holds that

$$f(x) \geq f(x_1) = \frac{(N-1)(N+1)}{2(L-1)}$$

which leads to the lower bound (7). □

Theorem 3. *By removing a link e, resulting in a graph $G-\{e\}$, the upper bound of the effective graph resistance $R_{G-\{e\}}$ of the reduced graph $G-\{e\}$ is*

$$\frac{R_{G-\{e\}}}{R_G} \leq \max_i \frac{\mu_i}{\mu_{i+1}}$$

where $i \in [1, N-2]$.

Proof.. Let $x_k = \frac{1}{\mu_j-\Delta\mu_j}$ and $a_k = \frac{1}{\mu_k}$ in inequality (6), then

$$\frac{1}{1-\min_i(\frac{\Delta\mu_i}{\mu i})} \leq \frac{\sum_{i=1}^{N-1}\frac{1}{\mu_i-\Delta\mu_i}}{\sum_{i=1}^{N-1}\frac{1}{\mu_i}} \leq \frac{1}{1-\max_i(\frac{\Delta\mu_i}{\mu_i})} \tag{12}$$

After a link removal, the interlacing property [7] shows that,

$$\mu_{i+1} \leq \mu_i - \Delta\mu_i \leq \mu_i \tag{13}$$

where $i = 1, 2, \ldots, N-1$. Subtracting μ_i on both sides of (13) leads to

$$0 \leq \Delta\mu_i \leq \mu_i - \mu_{i+1} \tag{14}$$

Substituting (14) into the right-hand side of (12) yields

$$\begin{aligned}\frac{1}{1-\max_i(\frac{\Delta\mu_i}{\mu_i})} &\leq \frac{1}{1-\max_i(\frac{\mu_i-\mu_{i+1}}{\mu_i})} \\ &= \frac{1}{1-(1-\min_i(\frac{\mu_{i+1}}{\mu_i}))} \\ &= \frac{1}{\min_i(\frac{\mu_{i+1}}{\mu_i})} = \max_i(\frac{\mu_i}{\mu_{i+1}})\end{aligned}$$

Based on definition (1) of the effective graph resistance, we establish the theorem. □

Figure 2 shows the probability that $\frac{\mu_i}{\mu_{i+1}}$ has a maximum at the index i within 10^3 instances of Erdős-Rényi and Barabási-Albert graphs, respectively. Figure 2a shows that $\frac{\mu_i}{\mu_{i+1}}$ has a maximum at $i = N-2$ with a probability higher than 0.5. Figure 2b shows that $\frac{\mu_i}{\mu_{i+1}}$ has a maximum at $i = 1$ with a probability 0.35. In both Figure 2a and 2b, the maximum of $\frac{\mu_i}{\mu_{i+1}}$ is attained within several highest and lowest values of the index i. Figure 3 shows the upper and lower bounds of the effective graph resistance $R_{G-\{e\}}$ from Theorem 2 and 3.

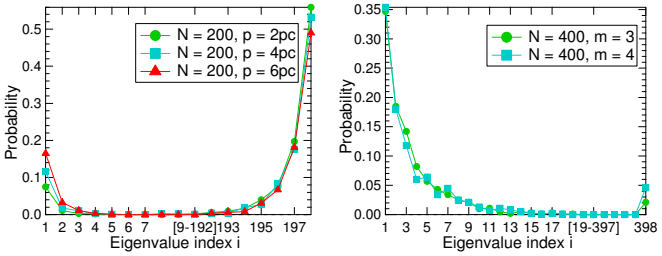

(a) Erdős-Rényi graph (b) Barabási-Albert graph

Fig. 2: The probability that $\frac{\mu_i}{\mu_{i+1}}$ has a maximum at the index i in Erdős-Rényi and Barabási-Albert graphs.

4 Optimization of the effective graph resistance

This section introduces four strategies for selecting a link whose addition minimizes the effective graph resistance and for protecting a link whose removal maximizes the effective graph resistance. The strategies are evaluated by comparing with the optimal effective graph resistance obtained by exhaustive search.

4.1 Strategies for Link Addition and Removal

In an exhaustive search, the optimal link l_{R^+} added between two nodes is discovered by checking all the possible links L_c. Similarly, the optimal link l_{R^-} is determined among all the possible links L.

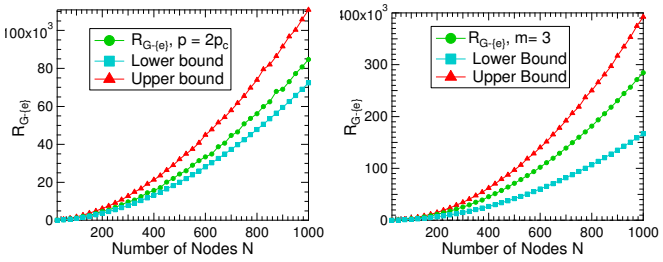

(a) Erdős-Rényi graph (b) Barabási-Albert graph

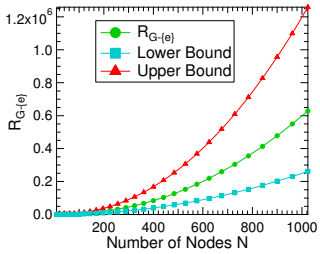

(c) Square lattice graph

Fig. 3: Upper and lower bounds of the effective graph resistance $R_{G-\{e\}}$.

An exhaustive search is computationally expensive as the number of nodes increases. More specifically, exhaustive search has a complexity order $O(N^5)$. This is computed by the computational order $\binom{N}{2} - L_c$ for checking all possible links multiplied by the order $O(N^3)$ for computing the pairwise effective resistance as illustrated in detail in Section 4.1.4. Strategies that determine the added or removed link based on topological and spectral properties of a network, provide a trade-off between a scalable computation and a high decrease or increase in the effective graph resistance. This section illustrates four strategies from which three of them are introduced in earlier work [21,22], yet none of these strategies are evaluated for the effective graph resistance.

A strategy S_s, $s \in \{1, 2, 3, 4\}$, defines a link $e = i \sim j$, where e does not already exist under link addition and e already exists under link removal. The selection criteria of nodes i and j for each strategy are illustrated in the rest of this subsection. In this paper, strategies S_1, S_2 are topological strategies and S_3, S_4 are spectral strategies.

4.1.1 Semi-random - strategy S_1

The node i has the minimum degree $\min(d_i)$ and node j is randomly chosen as $rand\{1, ..., L_c\}$.

The complexity of strategy S_1 is $O(N^2 - N + L_c + 1)$ computed as follows: (i) $O(N(N-1))$ is for counting the degrees of all the nodes. (ii) $O(L_c)$ is for finding the node i with minimum degree. (iii) $O(1)$ is for finding a random node.

4.1.2 Degree product - strategy S_2

The nodes i and j have the minimum[7] product of degrees $\min(d_i d_j)$. If there are multiple node pairs with the same minimum product of degrees, one of these pairs is randomly chosen.

The complexity of strategy S_2 is $O(N^2 - N + 2L_c)$ computed as follows: (i) $O(N(N-1))$ is for counting the degrees of all the nodes. (ii) $O(L_c)$ is for computing $d_i d_j$ for L_c unconnected node pairs. (iii) $O(L_c)$ is for finding the minimum product $d_i d_j$.

4.1.3 Fiedler vector - strategy S_3

The nodes i and j correspond to the i^{th} and j^{th} components of the Fiedler vector y that satisfy $\Delta y = \max(|y_i - y_j|)$, where $|y_i - y_j|$ is the absolute difference between the i^{th} and j^{th} components of the Fiedler vector y.

For strategy S_3, the complexity is $O(N^3 + 2L_c)$ computed as follows: (i) $O(N^3)$ is for computing the Fiedler vector y_i assuming the adoption of the QR algorithm [23] for computation. (ii) $O(L_c)$ is for computing $|y_i - y_j|$ for L_c unconnected node pairs. (iii) $O(L_c)$ is for finding the maximum of the difference $|y_i - y_j|$.

4.1.4 Effective resistance - strategy S_4

The nodes i and j have the highest effective resistance $\max(R_{ij})$. The pairwise effective resistance R_{ij} can be calculated as $R_{ij} = (\widehat{Q}^{-1})_{ii} + (\widehat{Q}^{-1})_{jj} - 2(\widehat{Q}^{-1})_{ij}$, where $\widehat{Q}^{-1}$ is the Moore-Penrose pseudoinverse [7] of Q.

For strategy S_4, the complexity is $O(N^3 + 4L_c)$ computed as follows: (i) $O(N^3)$ is for computing $\widehat{Q}^{-1}$. (ii) $O(3L_c)$ is for computing R_{ij} for L_c unconnected node pairs. (iii) $O(L_c)$ is for finding the maximum R_{ij}.

In case of link removals, L_c is replaced with L in all the four strategies. Table 2 summarizes all the strategies that add or remove a link $e = i \sim j$ and the order of their corresponding computational complexity.

	Node i	Node j	Complexity Order
S_1	$\arg\min_i(d_i)$	$rand\{1,..., L_c \text{ or } L\}$	$O(N^2)$
S_2	$\arg\min_{i,j}(d_i d_j)$		$O(N^2)$
S_3	$\arg\max_{i,j}(\lvert y_i - y_j \rvert)$		$O(N^3)$
S_4	$\arg\max_{i,j}(R_{ij})$		$O(N^3)$

Table 2: A summary of the strategies and the order of their computational complexity.

[7] Adding a link between nodes with the highest degree is evaluated as well. However, the performance is low and therefore this choice is not illustrated in this paper.

The strategies illustrated in this paper are indicative of a large number of other possible strategies. For example, two other strategies are tested:
S_5: The nodes i and j have the minimum product of closeness centrality $\min(cc_i cc_j)$. The closeness of a node i, $cc_i = \left[\sum_{j\neq i, j\in G} H_{ij}\right]^{-1}$, is computed as the inverse of the sum of hopcounts H_{ij} from a node i to each node j.
S_6: The nodes i and j correspond to the i^{th} and j^{th} components of the principal eigenvector x_1 that have the maximum product $\max((x_1)_i(x_1)_j)$ of the eigenvector components. The principal eigenvector x_1 belongs to the highest eigenvalue of the adjacency matrix.

Strategy S_5 has higher complexity than S_1 and has approximately the same performance with S_1 for link addition. Strategy S_6 has the lowest performance under link addition and has approximately the same performance with S_2 for link removal. The rest of this paper focuses on the four main strategies illustrated in this section.

4.2 Strategy Evaluation

The strategies are implemented and evaluated in MATLAB R2012b. First, the optimal effective graph resistance R^* is obtained by applying exhaustive search. Second, the effective graph resistance R_{S_s} is computed by adding or removing a link under each strategy $s \in \{1, 2, 3, 4\}$. Third, the absolute relative difference, $R_{D_s} = \left|\frac{R_{S_s}-R^*}{R^*}\right|$ and the probability $\Pr[R_{D_s} \geqslant x]$, where $x \in [\min(R_{D_s}), \max(R_{D_s})]$, evaluate the performance of the four strategies. The lower the probability is, the closer R_{S_s} is to R^* and the more effective the strategy is. The average difference $E[R_{D_s}] = \int_0^\infty \Pr[R_{D_s} \geqslant x]\, dx$ computed by the area under the curve of the probability distribution, indicates the average performance of the strategies.

4.2.1 Erdős-Rényi random graph

Figure 4 illustrates the performance of the four strategies in Erdős-Rényi random graphs. The figure is split into two subgraphs (a), (b), concerning link addition and removal. Figure 4a demonstrates that strategy S_4 is superior to all other strategies. Strategy S_2 outperforms strategy S_3 and strategy S_1 has the lowest performance. In Figure 4a, the average difference $E[R_{D_s}]$ for strategies S_1, S_2, S_3, S_4 is 2.99×10^{-3}, 0.24×10^{-3}, 0.36×10^{-3}, 0.04×10^{-3}.

Figure 4b shows that strategy S_4 is superior to S_3 and S_1. Compared to the second highest performance in Figure 4a, strategy S_2 has the lowest performance. The average difference $E[R_{D_s}]$ of strategies S_1, S_2, S_3, S_4 is 1.26×10^{-4}, 4.39×10^{-4}, 1.31×10^{-4}, 1.01×10^{-4}.

4.2.2 Barabási-Albert power law graph

Figure 5 illustrates the performance of the four strategies in Barabási-Albert power law graphs. Strategy S_4 achieves

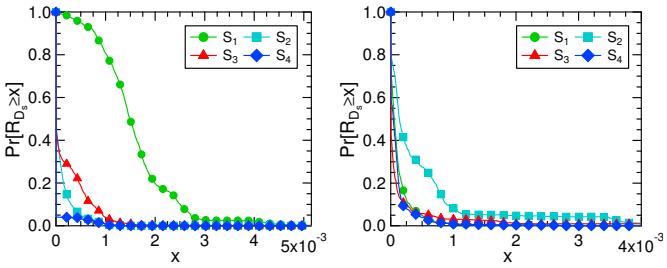

(a) Link Addition (b) Link Removal

Fig. 4: $\Pr[R_{D_s} \geqslant x]$ for each strategy S_s, $s \in \{1, 2, 3, 4\}$ in the Erdős-Rényi random graph with $N = 100$, $p = 2p_c$.

the highest performance in Figure 5a. Strategy S_3 outperforms strategies S_1 and S_2. The average difference $E[R_{D_s}]$ in Figure 5a for strategies S_1, S_2, S_3, S_4 is 1.74×10^{-3}, 1.69×10^{-3}, 0.29×10^{-3}, 0.01×10^{-3}.

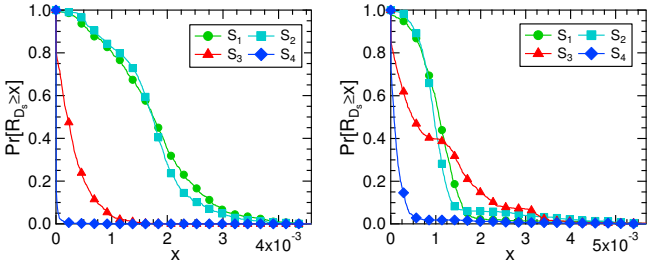

(a) Link Addition (b) Link Removal

Fig. 5: $\Pr[R_{D_s} \geqslant x]$ for each strategy S_s, $s \in \{1, 2, 3, 4\}$ in the Barabási-Albert power law graph with $N = 200$, $m = 3$.

Figure 5b shows strategy S_4 has the highest performance. The performance curve for S_3 crosses the curves for S_2 and S_1. Strategies S_2 and S_1 have comparable performance. The average difference $E[R_{D_s}]$ for strategy S_4 is 0.17×10^{-3}. For strategy S_3, the average difference $E[R_{D_s}]$ is 0.95×10^{-3} compared to 1.09×10^{-3} for strategies S_2, S_1, which indicates that strategy S_3 slightly outperforms S_2, S_1.

4.2.3 Watts-Strogatz small-world graph

Figure 6 illustrates the performance of the four strategies in the Watts-Strogatz small-world graphs. In contrast to the results for Erdős-Rényi and Barabási-Albert, strategy S_3 outperforms strategy S_4 in both Figure 6a and 6b. Strategy S_1 is superior to S_2 in Figure 6a, while the opposite holds in Figure 6b.

The average difference $E[R_{D_s}]$ for strategies S_1, S_2, S_3, S_4 in Figure 6a is 22.7×10^{-3}, 26.4×10^{-3}, 0.34×10^{-3}, 2.75×10^{-3}. These values in Figure 6b are 1.34×10^{-2}, 1.33×10^{-2}, 0.10×10^{-2}, 0.23×10^{-2}.

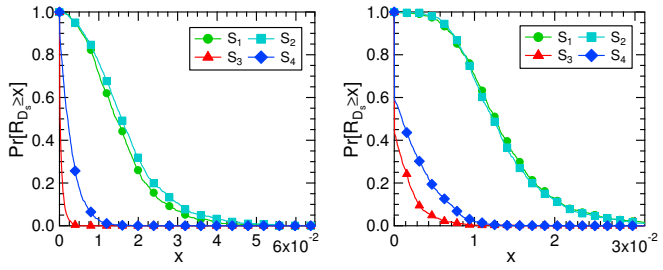

(a) Link Addition (b) Link Removal

Fig. 6: $\Pr[R_{D_s} \geqslant x]$ for strategy S_s, $s \in \{1, 2, 3, 4\}$ in the Watts-Strogatz small world graph with $N = 100$, $k = 6$ and $p = 0.1$.

4.2.4 Real-world networks

Table 3 illustrates the performance of the four strategies in real-world networks. The table is ordered by the number of nodes in the network. The optimal added link by exhaustive search is not calculated because of the high computational complexity. Using Western States Power Grid Network as an example, the number of possible added links is 1.2×10^7. Therefore, the four strategies are evaluated by comparing the value of the effective graph resistance: the lower the effective graph resistance after link addition or the higher the effective graph resistance after link removal, the more effective the strategy.

For a given network, for example the *Dutch Soccer Network* in Table 3, the effective graph resistance of strategy S_3 is 0.1318 that is the lowest one compared to the effective graph resistance of S_1, S_2 and S_4. Strategy S_3 outperforms strategies S_1, S_2 and S_4. For all the listed networks except the *Western European Railway Network* in Table 3, S_3 has the lowest effective graph resistance and outperforms the other three strategies. In contrast, the strategy S_4 outperforms strategy S_3 in *Western European Railway Network*. Strategy S_4 has the same performance as strategy S_3 in *Protein-Protein Interaction Network* and *Citation Network*.

Name	N	L	R_{S_1}	R_{S_2}	R_{S_3}	R_{S_4}
Coauthorship	379	914	2.05	2.04	1.95	1.96
Protein	529	535	49.5	69.7	36.8	36.8
Dutch Soccer	685	10310	0.132	0.132	0.131	0.132
Citation	2678	10368	0.823	0.823	0.819	0.819
Power Grid	4941	6594	2.03	2.04	1.95	1.96
Railway	8710	11332	18.2	19.0	17.4	17.3

Table 3: The effective graph resistance of the four strategies after link addition in real-world networks.

Table 4 shows the effective graph resistance of the four strategies under link removal. The infinite value of the effective graph resistance indicates that the removal of the selected link by a strategy disconnects the network. Strategy S_4 has the highest performance in all the listed networks. Strategy S_3 has comparable performance in *Protein-Protein Interaction Network*, *Dutch Soccer* and *Citation Network*.

Name	N	L	R_{S_1}	R_{S_2}	R_{S_3}	R_{S_4}
Coauthorship	379	914	2.08	2.07	2.21	∞
Protein	529	535	∞	∞	∞	∞
Dutch Soccer	685	10310	0.133	0.133	0.133	0.133
Citation	2678	10368	0.824	0.824	∞	∞
Power Grid	4941	6594	5.22	5.22	5.76	∞
Railway	8730	11332	19.0	19.0	19.4	∞

Table 4: The effective graph resistance of the four strategies after link removal in real-world networks.

4.2.5 Performance Overview

Table 5 shows the ranking of the four strategies according to their performance. Strategy S_4 has the highest performance for both link addition and removal in Erdős-Rényi and Barabási-Albert graphs. In contrast, strategy S_3 has the highest performance in Watts-Strogatz graphs under link addition and removal. Results are consistent with the larger graphs with number of nodes up to 400. In real world networks, either strategy S_3 or strategy S_4 has the highest performance for link addition and removal.

	Link Addition				Link Removal			
Rank / Network	1	2	3	4	1	2	3	4
Erdős-Rényi	S_4	S_2	S_3	S_1	S_4	S_1	S_3	S_2
Barabási-Albert	S_4	S_3	S_2	S_1	S_4	S_3	S_2	S_1
Watts-Strogatz	S_3	S_4	S_1	S_2	S_3	S_4	S_2	S_1
Real-world	S_3 or S_4		S_1 or S_2		S_3 or S_4		S_1 or S_2	

Table 5: The ranking of the four strategies according to their performance.

Despite the lower performance of strategies S_1 and S_2, their computational complexity is much lower compared to strategies S_3 and S_4. Therefore, the set of all strategies provides a trade-off between a low changing value of effective graph resistance and low computational complexity. Strategies S_1 and S_2 can be chosen when the computational resources are limited. Assuming that the computation of the optimal R^* is not an option for large networks, strategies S_3 and S_4 can be chosen under two scenarios: (i) In case of long term investments on infrastructural networks, such as railway networks, in which a link addition or removal is a costly operation and a strategy close to optimal R^* is a requirement. (ii) In case when the option of parallel computations, e.g. with MapReduce [24], is possible.

5 Effective Graph Resistance vs Algebraic Connectivity

The spectral expression of the effective graph resistance includes all the non-zero Laplacian eigenvalues, whereas the algebraic connectivity is one of the $N-1$ Laplacian eigenvalues. This section introduces a novel approach to compare the optimal links l_{R^+}, l_{α^+} and l_{R^-}, l_{α^-}. The comparison includes the probability that two optimal links are the same and the distance between the two optimal links in the corresponding line graph.

5.1 Probability of the same optimal link

Table 6 illustrates the probability $\Pr[l_{R^+} = l_{\alpha^+}]$ that l_{R^+} equals l_{α^+} in the 10^3 instances of Erdős-Rényi and Barabási-Albert graphs[8]. All the optimal links are obtained by exhaustive search. Table 6 illustrates that the maximum probability $\Pr[l_{R^+} = l_{\alpha^+}]$ obtained for Erdős-Rényi graph is 0.139 and for Barabási-Albert graph is 0.105. The optimal link for the algebraic connectivity is different from the optimal link for the effective graph resistance in most cases.

Erdős-Rényi	Probability	Barabási-Albert	Probability
$G_{2p_c}(50)$	0.139	$N = 100$, $m = 3$	0.034
$G_{2p_c}(100)$	0.102	$N = 100$, $m = 4$	0.105
$G_{2p_c}(200)$	0.074	$N = 200$, $m = 3$	0.013
$G_{4p_c}(200)$	0.068	$N = 200$, $m = 4$	0.066

Table 6: The probability $Pr[l_{R^+} = l_{\alpha^+}]$ in Erdős-Rényi and Barabási-Albert graphs.

Table 7 illustrates the probability $\Pr[l_{R^-} = l_{\alpha^-}]$ under link removal in the 10^3 instances of Erdős-Rényi and Bárabasi-Alber graphs. In contrast to the results in Table 6, the probability $\Pr[l_{R^-} = l_{\alpha^-}]$ is higher than 0.6 in Erdős-Rényi graph with link density $p = 2p_c$. However, when the link density p increases to $4p_c$, the probability $\Pr[l_{R^-} = l_{\alpha^-}]$ drops to approximately zero. One explanation is that the number of links in graph G increases with the increase of link density. The probability of choosing two links among all the possibilities decreases. The maximum probability $\Pr[l_{R^-} = l_{\alpha^-}]$ is 0.504 in Barabási-Albert graph. The decrease of the probability $\Pr[l_{R^-} = l_{\alpha^-}]$ with the increase of link density is also observed.

5.2 Proximity of optimal links

This subsection illustrates how the distance between the optimal links l_{R^+} and l_{α^+} is computed when l_{R^+} is different from l_{α^+}. The hopcount in the corresponding line graph is proposed as a measure of the distance between the two optimal links l_{R^+} and l_{α^+}. Table 8 shows the average hopcount $E[H]$ between nodes n_{R^+} and n_{α^+} in the line graphs. In the line graphs of Erdős-Rényi graphs, the average hopcount between n_{R^+} and n_{α^+} approximates 1 that means the links l_{R^+} and l_{α^+} share a node in the original graph on average. The average hopcount between n_{R^+} and n_{α^+} in the line graphs of Barabási-Albert graphs approximates 2. From the definition of line graph, it can be derived that the end nodes of l_{R^+} and l_{α^+} are different but one of the end nodes of l_{R^+} is adjacent to one of the end nodes of l_{α^+}. Table 8 indicates that the optimal link for the algebraic connectivity is in a proximity of 1 or 2 hops to the optimal link for the effective graph resistance. This distance corresponds to $25\% - 40\%$ of the graph diameter.

Erdős-Rényi	Probability	Barabási-Albert	Probability
$G_{2p_c}(50)$	0.677	$N = 100$, $m = 3$	0.504
$G_{2p_c}(100)$	0.665	$N = 100$, $m = 4$	0.208
$G_{2p_c}(200)$	0.613	$N = 200$, $m = 3$	0.460
$G_{4p_c}(200)$	0.002	$N = 200$, $m = 4$	0.113

Table 7: The probability $Pr[l_{R^-} = l_{\alpha^-}]$ in Erdős-Rényi and Barabási-Albert graphs.

Erdős-Rényi	$E[H]$	Barabási-Albert	$E[H]$
$G_{2p_c}(50)$	0.987	$N = 100$, $m = 3$	1.759
$G_{2p_c}(100)$	1.002	$N = 100$, $m = 4$	1.636
$G_{2p_c}(200)$	1.001	$N = 200$, $m = 3$	2.285
$G_{4p_c}(200)$	0.998	$N = 200$, $m = 4$	2

Table 8: The average hopcount $E[H]$ between l_{R^+} and l_{α^+} in the Erdős-Rényi and Barabási-Albert graphs.

As shown in Table 9, the average hopcount between n_{R^-} and n_{α^-} under link removal is lower than the average hopcount under link addition. For example, the $E[H]$ between n_{R^-} and n_{α^-} is 0.584 compared to 1.001 between n_{R^+} and n_{α^+} in Erdős-Rényi graph $G_{2p_c}(200)$. This observation is also confirmed by the fact that $\Pr[l_{R^-} = l_{\alpha^-}]$ is higher than $\Pr[l_{R^+} = l_{\alpha^+}]$.

Erdős-Rényi	$E[H]$	Barabási-Albert	$E[H]$
$G_{2p_c}(50)$	0.537	$N = 100$, $m = 3$	1.269
$G_{2p_c}(100)$	0.517	$N = 100$, $m = 4$	1.628
$G_{2p_c}(200)$	0.584	$N = 200$, $m = 3$	1.568
$G_{4p_c}(200)$	1.334	$N = 200$, $m = 4$	1.916

Table 9: The average hopcount $E[H]$ between l_{R^-} and l_{α^-} in the Erdős-Rényi and Barabási-Albert graphs.

Figure 7 illustrates the distribution of the hopcount $H(n_{R^+}, n_{\alpha^+})$ between the node n_{R^+} and n_{α^+} in the line graph of the Erdős-Rényi and Barabási-Albert graphs. In Figure 7a, the probability $\Pr[H(n_{R^+}, n_{\alpha^+})]$ is maximized for $H(n_{R^+}, n_{\alpha^+}) = 1$. The probability $\Pr[H(n_{R^+}, n_{\alpha^+}) >$

[8] Results for the Watts-Strogatz small-world graphs are not included to keep the illustrations more compact. However, these results are available upon request

1] converges to zero in $2-3$ extra hops, especially for large N. In Figure 7b, the probability $\Pr[H(n_{R^+}, n_{\alpha^+})]$ is maximized for $H(n_{R^+}, n_{\alpha^+}) = 1$ and converges to zero for $H(n_{R^+}, n_{\alpha^+}) = 5$.

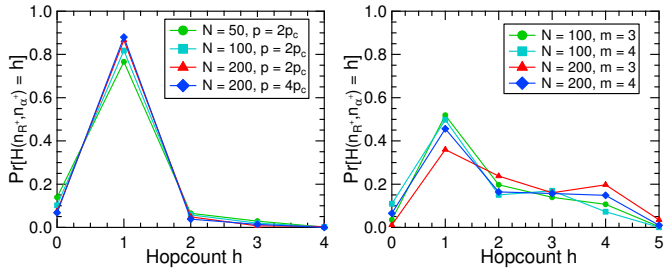

(a) Erdős-Rényi graph (b) Barabási-Albert graph

Fig. 7: The distribution of the hopcount $H(n_{R^+}, n_{\alpha^+})$ in the line graph G^* between the node n_{R^+} and the node n_{α^+}.

Figure 8 illustrates the distribution of the hopcount $H(n_{R^-}, n_{\alpha^-})$ between the node n_{R^-} and n_{α^-} under link removal. In Figure 8a, the probability $\Pr[H(n_{R^-}, n_{\alpha^-})]$ is maximized for $H(n_{R^-}, n_{\alpha^-}) = 0$ with link density $p = 2p_c$. when link density p increases, the peak of the probability shifts from 0 to 1. The probability $\Pr[H(n_{R^-}, n_{\alpha^-}) > 1]$ converges to zero in $2-3$ extra hops. In Figure 8b, the peak of the probability $\Pr[H(n_{R^-}, n_{\alpha^-})]$ shifts from 0 to 1 as the average degree grows and the probability $\Pr[H(n_{R^-}, n_{\alpha^-}) > 1]$ converges to zero at $H(n_{R^-}, n_{\alpha^-}) = 5$.

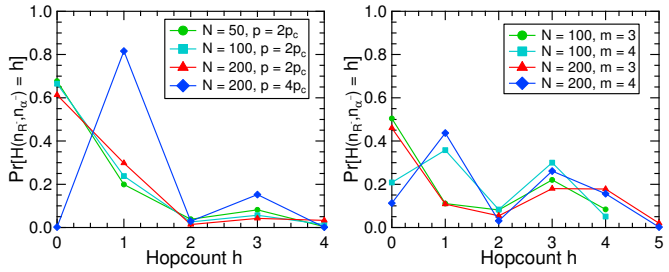

(a) Erdős-Rényi graph (b) Barabási-Albert graph

Fig. 8: The distribution of the hopcount $H(n_{R^-}, n_{\alpha^-})$ in the line graph G^* between the node n_{R^-} and the node n_{α^-}.

6 Comparison with Related Work

Network robustness is mostly studied under topological perturbations that usually concern (i) addition of nodes or links, (ii) removal of nodes or links, (iii) rewiring of links. These perturbations influence the spectral properties of networks. For example, Takamitsu *et al.* [25] study the influence of node removal on the second lowest Laplacain eigenvalue. Attilio *et al.* [26] focus on the largest eigenvalue under links perturbations. Van Mieghem *et al.* [22] study the spectral radius under link removal, whereas, Li *et al.* [27] investigate the spectral radius under node removal. In contrast to the spectral methodologies that consider a singe eigenvalue, the effective graph resistance studied in this paper captures the information of all the eigenvalues and therefore it contains a broader range of spectral information about the network.

Various Internet protocols and applications transmit data packets via the shortest path between a source and destination. The effect of perturbations is studied by the changes of the shortest path length that is only one aspect influenced in the network. Holme *et al.* [28] introduce the average inverse length of shortest path as a measure of network robustness under perturbations. A higher shortest path length may result in slower information propagation in the network. This approach is limited to the evaluation of the changes on the shortest path length. However, effective graph resistance is a metric with a broader scope, e.g., power grid networks [29] in which power flows are transmitted via all possible paths besides the shortest path. In contrast to the measure of average shortest path length, the effective graph resistance is based on pairwise resistance that measures information of all the possible paths between a source and destination.

Furthermore, the study of topological perturbations in complex networks can be used for link prediction originated from information science. Link prediction refers to inferring added links in the near future or removed links from an observed network [30]. Link prediction is applied in recommendation systems such as friendship recommendations between two strangers in social networks [31]. Algorithms based on structural nodal properties, such as the number of common neighbors [32] and an ensemble of all paths [31] are proposed for link prediction. Compared to structural properties, spectral characteristics of nodes provide different insights for link prediction, such as the Fiedler vector and effective resistance proposed in the optimization strategies of this paper. Therefore, the link addition and removal strategies in this paper can be potentially used in this application domain.

7 Conclusion and Future Work

This paper shows that adding or removing single links in theoretical and real-world complex networks has a measurable impact on network robustness. This paper contributes theoretical and experimental findings that are applicable in real-world scenarios such as single-line installments in infrastructural networks or single-line protection against cyber-physical attacks. The upper and lower bounds introduced in this paper can be used to support policy and decision makers to choose a line to install or protect given certain operational costs. Future work should study such trade-offs in specific application domain such as power grids. Moreover, when computational cost for finding optimal links to add or remove is prohibitive, the topological

and spectral strategies studied in this paper can still indicate links resulting in high robustness. This paper also shows that if the optimal added or removed links for algebraic connectivity are known, then the respective links for effective graph resistance are different but in close proximity. Deriving analytically the optimal links of effective graph resistance given the optimal links of algebraic connectivity and vice versa, is a theoretical challenge to address in future work.

This research is supported by the China Scholarship Council (CSC) and by the project NWO RobuSmart: Increasing the Robustness of Smart Grids through distributed energy generation: a complex network approach, grant number 647.000.001.

A Bounds for α_G in terms of R_G

The analogy of inequality (10) is:

$$\frac{N-2}{\sum_{j=1}^{N-2}\frac{1}{\mu_j}} \leq \frac{1}{N-2}\sum_{j=1}^{N-2}\mu_j$$

Introducing the definition $S=\sum_{j=1}^{N-2}\frac{1}{\mu_j}$, with the sum of all the eigenvalues [7] satisfying $\sum_{j=1}^{N-1}\mu_j = 2L$, it follows that

$$\frac{N-2}{S} \leq \frac{2L-\mu_{N-1}}{N-2}$$

With the definitions $S=\frac{R_G}{N}-\frac{1}{\mu_{N-1}}$, $\alpha_G=\mu_{N-1}$ and by assuming a connected graph ($\mu_{N-1}>0$), it holds, for $N>2$

$$\alpha_G \leq 2L - \frac{(N-2)^2}{\frac{R_G}{N}-\frac{1}{\alpha_G}}$$

which is transformed into a quadratic inequality of α_G:

$$\frac{R_G}{N}\alpha_G^2 + ((N-2)^2 - 1 - 2L\frac{R_G}{N})\alpha_G + 2L \leq 0 \qquad (15)$$

In a factored form and by denoting $\frac{2LR_G}{N} = \widetilde{R_G}$, the quadratic inequality (15) is expressed as follows:

$$0 \geq \left(\alpha_G - \frac{\widetilde{R_G}-(N-1)(N-3)-\xi}{\widetilde{R_G}/L}\right) \times \left(\alpha_G - \frac{\widetilde{R_G}-(N-1)(N-3)+\xi}{\widetilde{R_G}/L}\right)$$

where $\xi = \sqrt{[\widetilde{R_G}-(N-3)^2][\widetilde{R_G}-(N-1)^2]}$ is the square-root of the discriminant. The lower bound (3), rephrased as $\widetilde{R_G} \geq (N-1)^2$, shows that $\widetilde{R_G}-(N-3)^2 > 0$ and $\widetilde{R_G}-(N-1)(N-3) > 0$, hence, ξ is real. Therefore, the quadratic equation in (15) has the following two real roots:

$$x_1 = \frac{\widetilde{R_G}-(N-1)(N-3)-\xi}{\widetilde{R_G}/L}$$

$$x_2 = \frac{\widetilde{R_G}-(N-1)(N-3)+\xi}{\widetilde{R_G}/L}$$

Vieta's formula indicates that the product of roots equals $x_1x_2 = \frac{2L}{\frac{R_G}{N}} > 0$ that results in both x_1 and x_2 being either positive or negative. Since $x_2 > 0$, the root x_1 is also positive. In summary, we deduce a new lower bound:

$$\alpha_G \geq L\left(1 - \frac{(N-1)(N-3)}{\widetilde{R_G}} - \sqrt{[1-\frac{(N-3)^2}{\widetilde{R_G}}][1-\frac{(N-1)^2}{\widetilde{R_G}}]}\right)$$

and an upper bound for the algebraic connectivity:

$$\alpha_G \leq L\left(1 - \frac{(N-1)(N-3)}{\widetilde{R_G}} + \sqrt{[1-\frac{(N-3)^2}{\widetilde{R_G}}][1-\frac{(N-1)^2}{\widetilde{R_G}}]}\right)$$

Figure 9 illustrates the lower and upper bounds of the algebraic connectivity α_G for Erdős-Rényi graphs with different link density p. As link density increases, the upper and lower bounds come closer. The bounds converge to the algebraic connectivity resulting in an equality for (15).

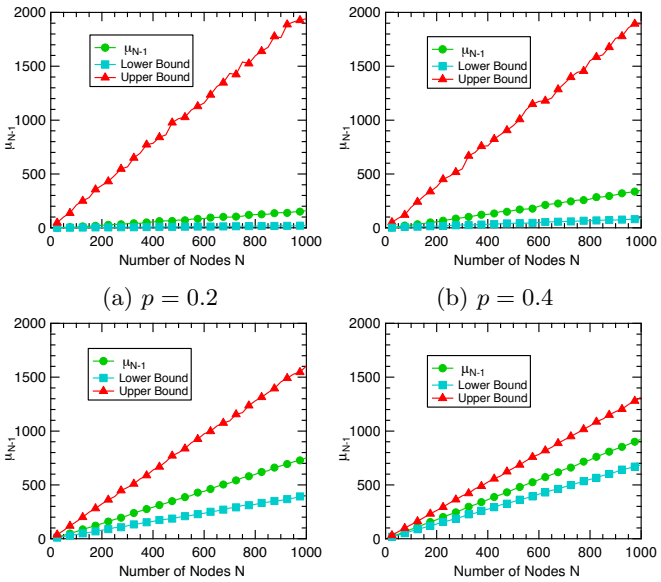

(a) $p = 0.2$ (b) $p = 0.4$

(c) $p = 0.8$ (d) $p = 0.95$

Fig. 9: Upper and lower bounds of the algebraic connectivity α_G.

References

1. W. Ellens, F.M. Spieksma, P. Van Mieghem, A. Jamakovic, R.E. Kooij, Lin. Algebra Appl. **435**, 2491 (2011)
2. A. Asztalos, S. Sreenivasan, B.K. Szymanski, G. Korniss, Eur. Phys. J. B **85**, 1 (2012)

3. W. Abbas, M. Egerstedt, *Robust graph topologies for networked systems*, in *3rd IFAC Workshop on Distributed Estimation and Control in Networked Systems* (2012), pp. 85–90
4. Y. Koç, M. Warnier, P. Van Mieghem, R.E. Kooij, F.M.T. Brazier, Physica A: Statistical Mechanics and its Applications **402**, 169 (2014)
5. A. Ghosh, S. Boyd, A. Saberi, SIAM Rev. **50**, 37 (2008)
6. P. Van Mieghem, X. Ge, P. Schumm, S. Trajanovski, H. Wang, Phys. Rev. E **82**, 056113 (2010)
7. P. Van Mieghem, *Graph spectra for complex networks* (Cambridge University Press, 2011)
8. M. Fiedler, Czech. Math. J. **23**, 298 (1973)
9. R. Grone, R. Merris, V.S. Sunder, SIAM J. Matrix Anal. Appl. **11**, 218 (1990)
10. P. Erdős, A. Rényi, Publ. Math. Debrecen **6**, 290 (1959)
11. P. Van Mieghem, *Performance analysis of communications networks and systems* (Cambridge University Press, 2006)
12. A.L. Barabási, R. Albert, science **286**, 509 (1999)
13. D.J. Watts, S.H. Strogatz, Nature **393**, 440 (1998)
14. M.E.J. Newman, S.H. Strogatz, D.J. Watts, Phys. Rev. E **64**, 026118 (2001)
15. L. da F. Costa, F.A. Rodrigues, G. Travieso, P.R. Villas Boas, Adv. Phys. **56**, 167 (2007)
16. R.E. Kooij, A. Jamakovic, F. van Kesteren, T. de Koning, I. Theisler, P. Veldhoven, Connections **29** (2009)
17. M.E.J. Newman, Phys. Rev. E **74**, 036104 (2006)
18. A. Jamakovic, S. Uhlig, Networks and Heterogeneous Media **3**, 345 (2008)
19. P. Gupta, P.R. Kumar, IEEE Trans. Inf. Theory **46**, 388 (2000)
20. R.K. Ganti, M. Haenggi, IEEE Trans. Inf. Theory **55**, 4067 (2009)
21. H. Wang, P. Van Mieghem, *Algebraic connectivity optimization via link addition*, in *Proceedings of the 3rd International Conference on Bio-Inspired Models of Network, Information and Computing Sytems* (ICST, 2008), p. 22
22. P. Van Mieghem, D. Stevanović, F. Kuipers, C. Li, R. Van De Bovenkamp, D. Liu, H. Wang, Phys. Rev. E **84**, 016101 (2011)
23. J.G.F. Francis, Comput. J. **4**, 332 (1962)
24. J. Dean, S. Ghemawat, Comm. ACM **51**, 107 (2008)
25. T. Watanabe, N. Masuda, Phys. Rev. E **82**, 046102 (2010)
26. A. Milanese, J. Sun, T. Nishikawa, Phys. Rev. E **81**, 046112 (2010)
27. C. Li, H. Wang, P. Van Mieghem, Lin. Algebra. Appl. **437**, 319 (2012)
28. P. Holme, B.J. Kim, C.N. Yoon, S.K. Han, Phys. Rev. E **65**, 056109 (2002)
29. F. Dörfler, F. Bullo, *Synchronization of power networks: Network reduction and effective resistance*, in *IFAC Workshop on Distributed Estimation and Control in Networked Systems* (2010), pp. 197–202
30. D. Liben-Nowell, J. Kleinberg, J. Am. Soc. Inform. Sci. Tech. **58**, 1019 (2007)
31. L. Lü, T. Zhou, Phys. Stat. Mech. Appl. **390**, 1150 (2011)
32. M.E.J. Newman, Phys. Rev. E **64**, 025102 (2001)